JCI insight

RESEARCH ARTICLE

Neutrophil extracellular traps promote macrophage inflammation and impair atherosclerosis resolution in diabetic mice

Tatjana Josefs,[1] Tessa J. Barrett,[1] Emily J. Brown,[1] Alexandra Quezada,[1] Xiaoyun Wu,[2] Maud Voisin,[3] Jaume Amengual,[2] and Edward A. Fisher[1,3]

[1]Division of Cardiology, Department of Medicine, New York University School of Medicine, New York, New York, USA. [2]Department of Food Science and Human Nutrition, University of Illinois, Urbana-Champaign, Illinois, USA. [3]Department of Microbiology, New York University School of Medicine, New York, New York, USA.

Neutrophil extracellular traps (NETs) promote inflammation and atherosclerosis progression. NETs are increased in diabetes and impair the resolution of inflammation during wound healing. Atherosclerosis resolution, a process resembling wound healing, is also impaired in diabetes. Thus, we hypothesized that NETs impede atherosclerosis resolution in diabetes by increasing plaque inflammation. Indeed, transcriptomic profiling of plaque macrophages from NET$^+$ and NET$^-$ areas in low-density lipoprotein receptor–deficient (*Ldlr*$^{-/-}$) mice revealed inflammasome and glycolysis pathway upregulation, indicating a heightened inflammatory phenotype. We found that NETs declined during atherosclerosis resolution, which was induced by reducing hyperlipidemia in nondiabetic mice, but they persisted in diabetes, exacerbating macrophage inflammation and impairing resolution. In diabetic mice, deoxyribonuclease 1 treatment reduced plaque NET content and macrophage inflammation, promoting atherosclerosis resolution after lipid lowering. Given that humans with diabetes also exhibit impaired atherosclerosis resolution with lipid lowering, these data suggest that NETs contribute to the increased cardiovascular disease risk in this population and are a potential therapeutic target.

Introduction

Cardiovascular disease (CVD) and diabetes are both associated with leukocytosis (1, 2). We and others have previously reported that hyperglycemia in mice impaired the resolution of atherosclerosis after lipid lowering (3, 4). Hyperglycemia also stimulated myelopoiesis in the mice, which increased circulating levels of monocytes and neutrophils and their entry into atherosclerotic plaques (5–7). While the contribution of monocyte-derived macrophages to atherogenesis has been extensively studied, less is known about neutrophils. Accumulating evidence indicates that neutrophils are also important protagonists in plaque progression (8). Their ability to form neutrophil extracellular traps (NETs) (9), structures found in human and mouse plaques (10–12), is of increasing interest in the context of atherogenesis due to the proinflammatory nature of NETs (13).

First reported in 2004 (14), NETosis is a process in which, in response to pathogens and sterile inflammatory stimuli, neutrophils release cytosolic and nuclear material forming a net-like extracellular structure (15). Relevant to atherogenesis, stimulators of NETosis include cholesterol crystals, oxidized low-density lipoprotein, oxysterols, platelets, and various chemokines (9). NETosis is not only stimulated by inflammation but can also promote it (9), for example, by increasing monocyte recruitment to inflamed sites and triggering macrophages to release reactive oxygen species and proinflammatory cytokines (16). The effects of NETs on plaque macrophages are thought to involve activation of their inflammasomes, but direct evidence in vivo to support this is scant (17).

In mice, genetic and pharmacological inhibition of NETosis reduces plaque size, inflammation, and features of instability (10, 18). In humans, circulating NET biomarkers positively correlate with atherosclerotic plaque size and are independently associated with clinical severity of CVD and the incidence of major adverse cardiac events (19, 20). One clinical population in which NETs are hypothesized to be particularly atherogenic is those with diabetes. Compared with people without diabetes, those with diabetes exhibit increased CVD risk and impaired atherosclerosis resolution, or plaque regression, after lipid-lowering

Authorship note: TJ and TJB contributed equally to this work.

Conflict of interest: EAF reports receiving income > $10,000 from being an expert witness on behalf of Amgen (PCSK9 antibodies) and Dr. Reddy's Laboratories (eicosapentaenoic acid).

Submitted: November 6, 2019
Accepted: March 11, 2020
Published: March 19, 2020.

Reference information: *JCI Insight*. 2020;5(7):e134796. https://doi.org/10.1172/jci.insight.134796.

therapy (21, 22). That NETs could be an important basis of these findings is supported by studies in which circulating NET biomarkers are correlated with both CVD and diabetes severity (23). Factors promoting NETosis in diabetes include both neutrophilia and hyperglycemia, which primes neutrophils for NET formation (24) and provides an increased substrate for NETosis, which is glucose dependent (25).

To date, CVD clinical studies have addressed the role of NETs only in the progression of atherosclerosis. Given that most patients, including those with diabetes, commence primary or secondary CVD prevention (typically lipid lowering) after the formation of plaques, resolution of atherosclerosis is an important, and largely unmet, clinical goal. The information presented above suggested to us that the failure of lipid-lowering therapies to fully reduce CVD risk in patients with diabetes, or to maximally resolve atherosclerosis in mice and patients with diabetes (reviewed in refs. 26–28), represented adverse consequences of the increased plaque level of NETs in this metabolic setting (25). This phenomenon would be similar to NETs impairing wound healing in diabetes (24).

Thus, we have investigated the effect of NETs on atherosclerosis resolution in mice with and without diabetes, using deoxyribonuclease 1 (DNase1) as a tool to deplete NETs from plaques (as in ref. 10). NETs had a direct proinflammatory influence on plaque macrophages, while DNase1-mediated depletion was associated with dampening of macrophage inflammation and improved atherosclerosis resolution after lipid lowering, despite ongoing hyperglycemia. Given that DNase1 has approved applications in other human diseases (e.g., cystic fibrosis), the results also suggest a mechanistic approach to improving atherosclerosis resolution in high-risk patients with diabetes, which remains an important clinical goal.

Results

NET formation is associated with a proinflammatory macrophage phenotype. Although NETs have been associated with macrophage activation and potentiating plaque formation (10), their molecular effects on plaque macrophage phenotype in vivo have not been directly determined. To address this gap, we collected macrophages ($CD68^+$ cells) in NET^+ and NET^- atherosclerotic plaque areas (Figure 1A and Supplemental Figure 1A; supplemental material available online with this article; https://doi.org/10.1172/jci.insight.134796DS1) by laser capture microdissection (LCM) in low-density lipoprotein receptor–deficient ($Ldlr^{-/-}$) mice after 16 weeks of Western diet feeding. Collected macrophages provided material for profiling by RNA-Seq to characterize the phenotypical features of macrophages in NET^+ areas in atherosclerotic plaques (Figure 1, B and C).

Consistent with a proinflammatory phenotype, glycolysis and inflammasome pathways were enriched in macrophages isolated from NET^+ areas relative to those in NET^- regions (Figure 1, D and E). Confirmation of inflammasome activation was determined by immunohistochemical staining for nod-like receptor family pyrin domain-containing 3 (NLRP3) and caspase-1 and quantification of their localization in NET^+ versus NET^- macrophage regions (Figure 1F). Inflammasome activation was found to be significantly associated with macrophages present in NET^+ areas ($P = 0.03$, Figure 1G). In addition to the enrichment in inflammasome-related genes in the NET^+ areas, the enrichment of glycolytic markers also indicates a switch to a proinflammatory M1-like macrophage phenotype (29). Indeed, based on standard markers, the $CD68^+$ cells from NET^+ versus NET^- areas were enriched in M1 (3.6-fold increase, inducible nitric oxide synthase [*inos*]) and suppressed in M2 (2-fold decrease [*Cd206*]). Further, immunofluorescence staining of iNOS confirmed increased proinflammatory macrophages in NET^+ plaque areas ($P = 0.055$, Figure 1H).

To exclude the possibility that the RNA from $CD68^+$ cells selected from NET^+ areas was contaminated by neutrophil RNA, we compared the reads for CD68 to those of the neutrophil markers lymphocyte antigen 6 complex locus G6D *(Ly6g),* myeloperoxidase *(Mpo*), and neutrophil elastase (*Ne*). Counts for CD68 were 7500-fold greater than those of neutrophil transcripts, confirming the specificity of our approach (Supplemental Figure 1B). Additionally, to exclude the possibility of significant contamination with vascular smooth muscle cells (VSMCs), which can take on characteristics of macrophages when cholesterol loaded in vitro (30) or in atherosclerotic plaques (31–33), we compared the transcript expression of *Cd68* to the myeloid-specific transcript *Ptprc* (*Cd45*) and the smooth muscle cell markers myosin heavy chain-11 (*Myh11)* and calponin 1 (*Cnn1)* using the expression values from RNA-Seq data obtained in the present study and in primary murine bone marrow–derived macrophage (BMDMs) and murine VSMCs. As shown in Supplemental Figure 1C, the *Cd45*/*Cd68* ratio was comparable between the laser-captured $CD68^+$ cells and BMDMs, whereas *Cd45* was undetectable in murine VSMCs. Further, compared with laser-captured $CD68^+$ cells, the *Myh11*/*Cd68* and *Cnn1*/*Cd68* ratios are approximately 12-fold higher in VSMCs. Overall, these data show that the data in Figure 1 are not confounded to a significant extent by contamination by

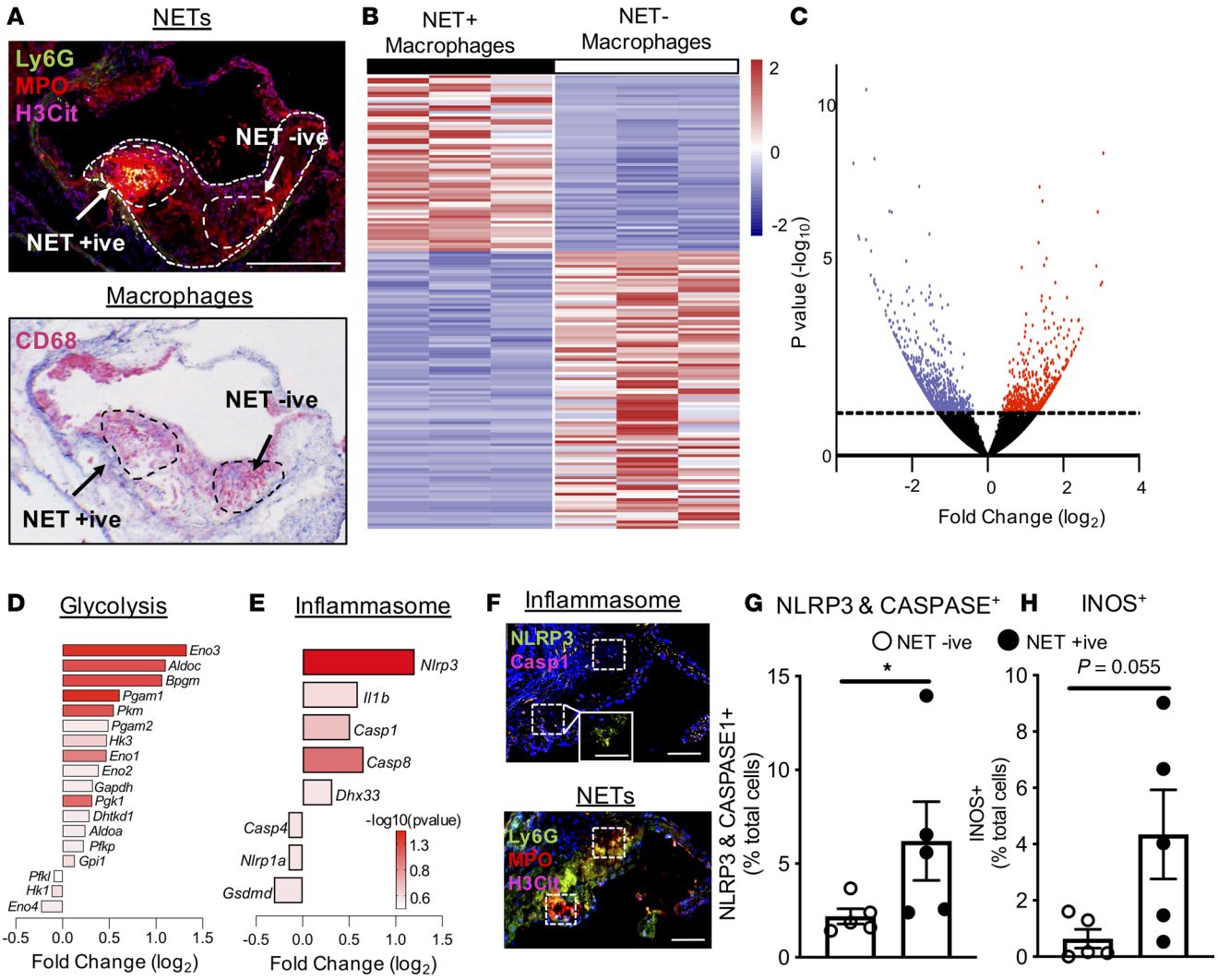

Figure 1. Neutrophil extracellular traps in atherosclerotic plaques skew macrophages to a proinflammatory phenotype. (**A**) Representative atherosclerotic plaque section stained for neutrophil extracellular traps (NETs), as determined by colocalization of myeloperoxidase (MPO), the lymphocyte antigen 6 complex locus G6D (Ly6G), citrullinated histone H3 (H3Cit), and macrophages (CD68). $CD68^+$ cells were collected via laser capture microdissection (LCM) in NET^+ and NET^- areas and sequenced. Scale bar: 100 μm. (**B**) Heatmap and (**C**) volcano plot showing differential gene expression in NET^+ versus NET^- macrophages. (**D**) Upregulation of the glycolysis and (**E**) inflammasome pathways in NET^+ compared with NET^- macrophages, as determined using Ingenuity Pathway Analysis. (**F**) Immunofluorescence staining and (**G**) quantification confirming the inflammasome pathway activation (nod-like receptor family pyrin domain-containing 3 [NLRP3]) in $NETs^+$ area. Scale bar: 50 μm. (**H**) Quantification of iNOS immunofluorescence staining showing an increase in iNOS in NET^+ versus NET^- areas (%DAPI). n = 3–5/group, $^*P < 0.05$ using unpaired t test.

other cell types and provide further support that NETs skew macrophages toward a proinflammatory phenotype in atherosclerotic plaques.

Clearing NETs can overcome impaired atherosclerosis resolution in diabetic mice. Neutrophils isolated from diabetic mice and humans are more prone to form NETs, with NET formation leading to impaired wound healing (24). We have also shown that, even with lipid lowering, maximal atherosclerosis resolution requires reduced macrophage inflammation (34). Thus, we hypothesized that the expected increase in plaque NETs in diabetic mice would impair atherosclerosis resolution due to their proinflammatory effects on macrophages (Figure 1) and that resolution in diabetic mice would improve by reducing NETs.

To test this, $Ldlr^{-/-}$ mice were fed a Western diet for 16 weeks to generate advanced atherosclerotic lesions, and atherosclerosis resolution was induced, as in a previous study (5), by feeding the mice a chow diet for 4 weeks, which resulted in decreased plasma lipid levels (Figure 2A and Table 1). A subset of mice were made diabetic by injection of streptozotocin (STZ). Since NETs are predominantly degraded by exonucleases (35), mice received DNase1 or vehicle injections every other day during the resolution period.

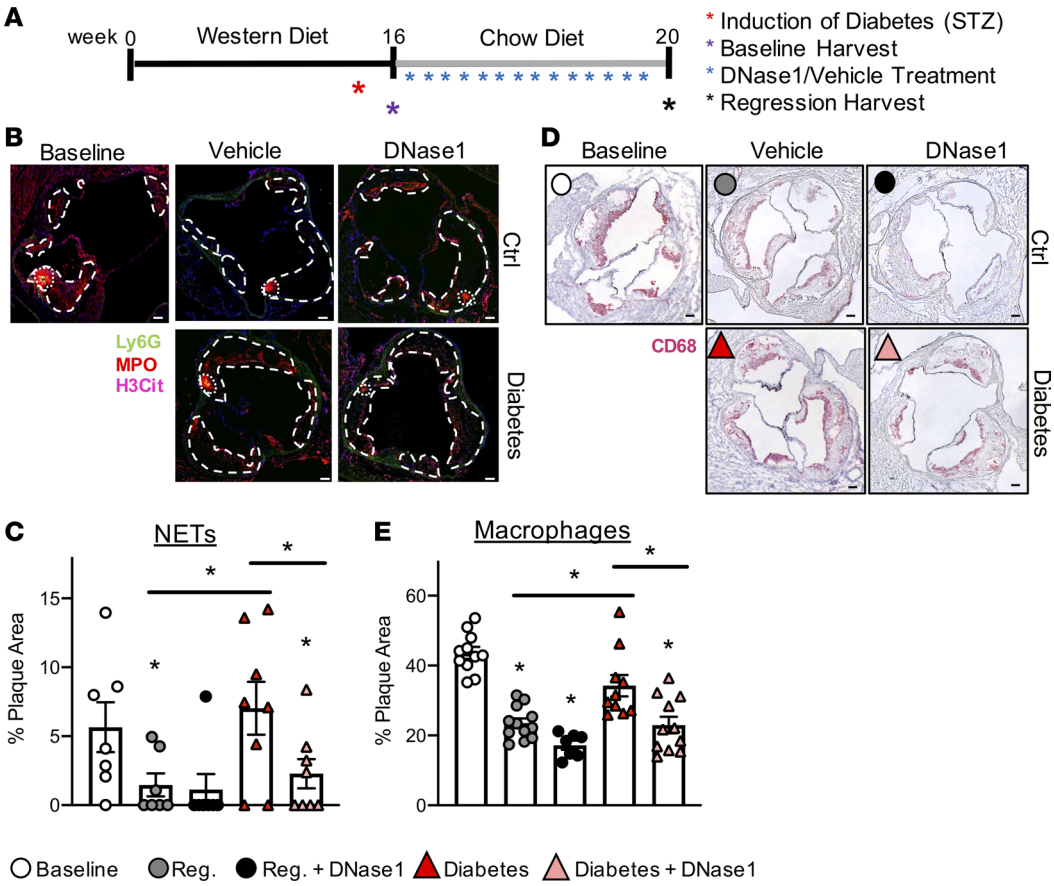

Figure 2. DNase1 treatment promotes atherosclerosis resolution in diabetic mice. (**A**) Male *Ldlr*$^{-/-}$ mice were fed a Western diet for 16 weeks to develop baseline plaques. At week 15, a subset of mice received streptozocin injections to induce diabetes. At week 16, a subset of mice were harvested for baseline measures, and all other mice were switched to a chow diet to induce resolution of plaques. These mice were then split into 2 groups and over a 4-week period received either DNase1 (62.5 μg/mouse) or vehicle injections every other day. At week 20, mouse tissues were harvested for plaque analyses. (**B**) NET staining and (**C**) quantification in aortic roots, as determined by composite staining of myeloperoxidase (MPO), the lymphocyte antigen 6 complex locus G6D (Ly6G), and citrullinated histone H3 (H3Cit). Scale bar: 100 μm. (**D**) Representative images and (**E**) quantification of CD68 staining as a marker of plaque macrophage content. Scale bar: 100 μm. Data are shown as mean ± SEM. n = 7–12/group, $^*P < 0.05$, 1-way ANOVA with Tukey's multiple comparison test.

In total, we compared baseline (mice sacrificed after 16 weeks on a Western diet) and 4 resolution groups: control, control + DNase1, STZ-induced diabetes, and diabetes + DNase1.

Neither STZ nor DNase1 affected total plasma cholesterol levels in the 4 resolution groups, with the levels in each significantly reduced when compared with those of baseline mice (Table 1). Plasma glucose levels were increased in the STZ groups only (Table 1). To evaluate NET content, we performed standard NET staining (MPO, citrullinated histone H3 [H3Cit] and the neutrophil marker Ly6G; Figure 2B) and quantified NETs as their percentage of plaque area (Figure 2C). Strikingly, in the nondiabetic mice, we observed a decrease in total plaque NET area in the control and DNase1 resolution groups when compared with baseline (5.7% vs. ~1.5% of plaque area), showing that NETs can resolve spontaneously in a nonhyperlipidemic environment. As expected, NETs did not resolve spontaneously in hyperglycemic conditions, but, notably, we observed a substantial decrease in NET content in the diabetes + DNase1 group (7.0% vs. 2.3% of plaque area, or a 68% reduction).

To determine if NET content correlated negatively with atherosclerosis resolution, CD68$^+$ macrophages were quantified and represented as the percentage of plaque area (%CD68; Figure 2, D and E). As expected, we found a significant decrease in lesion %CD68 in control mice compared with the baseline group (43.6 % vs. 24.1 %). Atherosclerosis resolution was unchanged in control mice receiving DNase1, consistent with the spontaneous loss of NETs in those mice. In diabetic mice, the reduction of %CD68

Table 1. Total plasma cholesterol and blood glucose levels

	Cholesterol (mg/dL)	Blood glucose (mg/dL)
Baseline	1000 ± 327.7	108.6 ± 32.3[A]
Regression	221.6 ± 71.1[B]	123.5 ± 31.3[A]
Regression + DNase1	216.4 ± 28.5[B]	175.0 ± 26.7[A]
Diabetes	325.1 ± 83.4[B]	450.5 ± 79.5
Diabetes + DNase1	323.3 ± 96.4[B]	453.8 ± 99.1

Mean ± SD. n = 5–13/group, 1-way ANOVA, [A]$P < 0.0001$ compared with diabetes, [B]$P < 0.0001$ compared with baseline.

immunostaining was impaired (43.6 % vs. 35.2 %), as expected (3). Notably, DNase1 treatment in diabetic mice showed significantly enhanced atherosclerosis resolution (35.2 % vs. 23.0 %), which was comparable to that of control mice.

To determine the relationships among the relative contributions to plaque characteristics by macrophages (above), extracellular matrix (as assessed by collagen), and necrotic core, additional plaque analyses were performed. As shown in Figure 3A, there was a significant reduction in plaque size in all of the resolution groups (Figure 3A) compared with that in baseline. Collagen content tended to increase relative to baseline, with statistical significance achieved in the resolution control group (Figure 3B). The necrotic core plaque areas were found to be similar in the baseline and the diabetes resolution groups and significantly lower in the other resolution groups, including DNase1-treated diabetic mice (Figure 3C).

DNase1 treatment reduces NET-induced plaque macrophage inflammation and promotes atherosclerosis resolution in diabetic mice. The results in Figure 2 showed that DNase1 treatment was able to overcome the impairment of atherosclerosis resolution by diabetes. Because a prominent feature of macrophages in NET$^+$ areas is the induction of the inflammasome and other metabolic and transcriptomic changes characteristic of inflammation (Figure 1), we hypothesized that the benefits of NET clearance in diabetic mice (Figure 2) were associated with a reduction in the inflammatory phenotype of plaque macrophages. Consistent with this, the percentage of macrophages associated with plaque NETs was significantly decreased by 90%, from 2.7 to 0.3%, in the DNase1-treated diabetic mice compared with that in diabetic mice with no treatment (Figure 4, A and B). To support this hypothesis more directly, we performed immunofluorescence staining of plaques for the inflammasome markers NLRP3 and caspase-1 (Figure 4C). Indeed, NLRP3$^+$ and caspase-1$^+$ cells were significantly increased in diabetic mice, compared with those in the control group, and decreased with DNase1 treatment. Additionally, the increase in plaques of diabetic mice of the inflammatory macrophage marker iNOS was reversed with DNase1 treatment (Figure 4D). As we previously reported (6, 7), there was a significant increase in circulating neutrophils in diabetes. There was also a trend toward increased plaque neutrophils (Supplemental Figure 2), with a suggestion that DNase1 reduced both increases.

Cholesterol crystals have been shown to be an inflammasome activator in atherosclerosis (36). Thus, we examined whether they were associated with the macrophage inflammation we observed and if

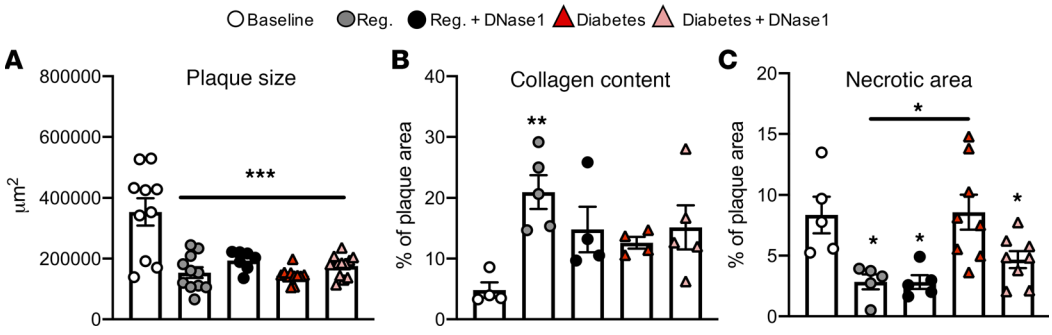

Figure 3. Effects of DNase1 treatment on plaque size, collagen content, and necrotic area in atherosclerotic plaques. More analyses of mice described in Figure 2. Quantification of (**A**) plaque size, (**B**) Picrosirius red staining to determine collagen content, and (**C**) plaque necrotic area. Data are shown as mean ± SEM. n = 4–12/group, *$P < 0.05$, ** $P < 0.005$, ***$P < 0.001$ 1-way ANOVA with Dunnett's multiple comparison test compared with the baseline (**A** and **B**) or diabetes (**C**) group.

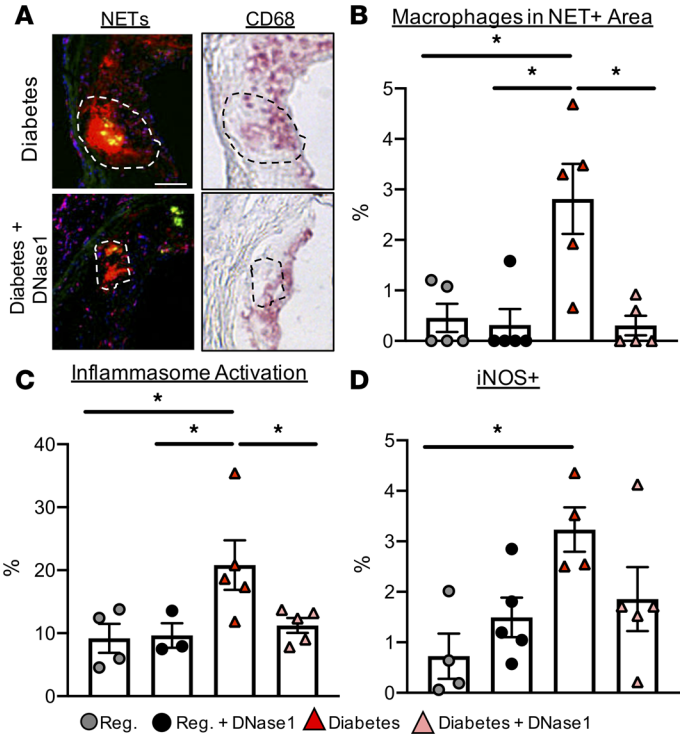

Figure 4. DNase1 treatment promotes atherosclerosis resolution in diabetic mice by reducing NETs-induced plaque macrophage inflammation. More analyses of mice described in Figure 2. (**A**) Overlapping NET (left) and CD68 staining (right) in diabetic mice versus diabetic mice treated with DNase1. Scale bar: 50 μm. (**B**) Percentage of macrophages colocalized with NETs. (**C**) Quantification of NLRP3$^+$ and caspase-1$^+$ cells and (**D**) iNos$^+$ cells, all as the percentage of DAPI staining of plaques. Data are shown as mean ± SEM. n = 3–5/group, *P < 0.05, 1-way ANOVA with Tukey's multiple comparison test.

DNase1 treatment affected their plaque content. Cholesterol crystals in atherosclerotic plaques were detected using polarized light (Figure 5A). As shown in Figure 5B, in the resolution groups, the cholesterol crystal content was approximately 70% greater (P = 0.01) in the diabetes (2.2%) versus control mice (1.3%). Interestingly, cholesterol crystals tended to be decreased in the diabetes + DNase1 group compared with that in the diabetes group (P = 0.06).

Discussion

NETs are found in human and mouse plaques, and in mice, they are associated with increased atherosclerosis progression (10–12). They have also been shown to impair wound healing in diabetic mice (24). Though considered to be generally inflammatory, how NETs contribute to macrophage activation is incompletely understood (17). The present study addresses this gap in knowledge. By isolation of macrophages from NET$^+$ and NET$^-$ plaque areas, we identified that NETs induce a proinflammatory "M1-like" macrophage phenotype, as evidenced at the molecular level by enriched transcripts characteristic of glycolysis and inflammasome activation and at the protein level by increases in relevant immunohistochemical markers. We also detected enhanced NET presence in diabetic plaques, consistent with a study in nonatherosclerotic mice that demonstrated that diabetes primes neutrophils for NET production (24).

The NET-macrophage interaction is a likely contributing factor to persistent macrophage inflammation in the plaques of diabetic mice, even after lipid lowering. This is supported by our current study, which found a reduction in plaque inflammation and proinflammatory macrophages in lesions of diabetic mice following the degradation of NETs with DNase1 in conjunction with lipid lowering. Further, we provide evidence that the resolution of plaque NETs in diabetic mice promotes a more stable appearance, as noted by a decrease in plaque necrotic area following DNase1 treatment. These data are consistent with the association between NET formation and human plaque instability (12, 37).

DNase1 reduces NETs by degradation of the chromatin fibers that comprise their backbone (14), which usually, but not always, reduces inflammation and disease severity in several models (38). Based on the results in the present study, we can add the resolution of atherosclerosis in diabetes to the list of conditions that are improved by reducing NET content. In addition to the direct effects in plaques by the reduction of NETs (e.g., reduced inflammasome activation in plaque macrophages), there are likely indirect benefits as well. For example, inflammation in plaques also increases neutrophil recruitment, further amplifying inflammation (39). This reasoning likely provides the logical link between the reduction in plaque inflam-

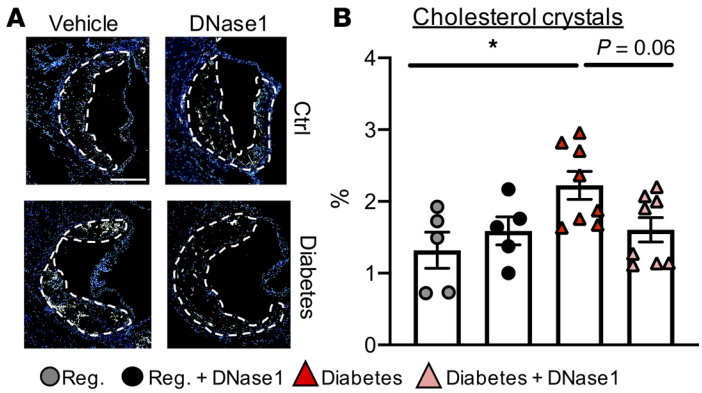

Figure 5. Effects of diabetes and DNAse1 treatment on cholesterol crystal content in resolving plaques. More analyses of mice described in Figure 2. (**A**) Cholesterol crystal visualization (white) and (**B**) quantification (as % plaque area) in atherosclerotic plaques with DAPI (blue) used as a counterstain. Scale bar: 100 μm. Data are shown as mean ± SEM. n = 5–8/group, $^*P < 0.05$, 1-way ANOVA with Tukey's multiple comparison test.

mation in diabetic mice (Figure 4) and the data suggesting that the increased circulating and plaque neutrophil levels in the diabetic mice were partially suppressed by DNase1 treatment (Supplemental Figure 2).

The present results showing a powerful effect of NETs on macrophage inflammasome activation led us to consider this finding in the context of another mediator of inflammasome activation in atherosclerosis, namely cholesterol crystals (36). The current understanding is that the inflammasome pathway requires two signals for full activation. Warnatsch et al. (10) have shown that NETs are a priming cue, with the second signal being cholesterol crystals (9). Furthermore, crystal formation and inflammasome activation were recently shown by Westerterp et al. to be promoted by reduced cholesterol efflux via ATP-binding cassette transporter A1/G1 (ABCA1/ABCG1) (40). Additionally, cholesterol crystals are not only the second signal for inflammasome activation, but they also stimulate NETosis (10).

As shown in Figure 5, cholesterol crystals were increased in diabetic mice relative to the other resolution groups, which is consistent with hyperglycemia reducing cholesterol efflux in macrophages and their precursors by decreasing ABCA1/ABCG1 expression (e.g., refs. 6, 7). Taken together, our data and the published data imply that cholesterol crystals could play a dual role in atherosclerosis, namely to promote NETosis, which provides multiple priming cues (first signals) for macrophage inflammasome activation, and also to serve as the second signal to complete the activation process in the primed macrophages. DNase1 treatment, by clearance of NETs, would reduce both types of macrophage inflammasome signals. This results in less macrophage inflammation, which we have shown is required to promote maximal atherosclerosis resolution after lipid lowering (34).

In summary, we have shown for the first time to our knowledge the molecular effect of NETs on plaque macrophages, especially on their inflammasome and glycolytic pathways. We also show that NETs formed during atherosclerosis progression in nondiabetic mice can spontaneously resolve upon the correction of hyperlipidemia. In contrast, they persist in the setting of diabetes and impair atherosclerosis resolution, likely due to their activation of macrophages and exacerbation of the general inflammatory environment in the plaque. Notably, DNase1 was an effective treatment to improve atherosclerosis resolution in the face of ongoing hyperglycemia. Because the rate of CVD remains higher in people with diabetes compared with those without diabetes after similar lipid lowering, the results suggest not only a basis for this, but also the therapeutic potential of NET reduction, especially in those whose diabetes is not well controlled.

Methods

Animals and atherosclerosis regression study. *Ldlr* $^{-/-}$ mice (The Jackson Laboratory) were fed Western diet (0.3% cholesterol; Dyets Inc. D101977Gi) for 16 weeks (progression), followed by 4 weeks (regression) on chow diet. STZ (MilliporeSigma, S0130-500 MG; 0.05 mg/g body weight) or sodium citrate (control) was injected daily for 5 days i.p. just before regression to induce diabetes, as described previously (7). During the 4-week regression period, DNase1 (62.5 μg/mouse Dornase Alfa, Genentech Inc.) in 0.9% NaCl or 0.9% NaCl only (control) was injected i.p. every other day. At the day of sacrifice, mice were anesthetized via i.p. injection of ketamine (100 mg/kg) and xylazine (10 mg/kg). Blood was collected via cardiac puncture

in EDTA-containing tubes, and mice were perfused with 10% sucrose in saline solution (0.9% NaCl). Collected aortic roots were embedded in optimal cutting temperature (OCT) compound and frozen at –80°C.

Plasma lipid and glucose measurements. Total cholesterol was measured using a Total Cholesterol E Kit (Wako Life Science, NC9138103). Plasma glucose levels were determined using the Contour Blood Glucose Monitoring System (Bayer).

Flow cytometry. Total white blood cell counts were measured from freshly collected mouse blood using a hematology cell counter (Oxford Science Inc.). Red blood cells were lysed with buffer (MilliporeSigma), and cells were stained with CD45 Pe/Cy7 (BioLegend, 103114), CD115 PE (BioLegend, 135505), and APC Ly-6G/Ly-6C (Gr-1, BioLegend, 108412). Neutrophils were identified by flow cytometry using LSRII analyzer and analyzed using FlowJo v10.

Atherosclerotic plaque assessment. Serial sections (6-μm thick) were stained for CD68 (rat anti-mouse CD68, Bio-Rad, MCA1957), as previously done (34). Briefly, sections were fixed and permeabilized with 100% ice-cold acetone, blocked, and stained with a rat anti-mouse CD68 antibody (Bio-Rad, MCA1957), followed by an incubation with a biotinylated rabbit anti-rat IgG secondary antibody (Vector Laboratories, BA4000), and visualized using the Vectastain ABC kit (Fisher Scientific, NC9313719). Slides were counterstained with H&E (MilliporeSigma), dehydrated in an ethanol gradient and xylene (Fisher Scientific), and mounted with coverslips using Permount (Fisher Scientific). NETs were identified using colocalization immunofluorescence staining of Ly6G (BD Bioscience, 551459), MPO (Abcam, ab90812), and H3Cit (Abcam, ab5103). Tissue was fixed in formalin and permeabilized using 0.5% Triton X-100, followed by incubation of primary antibody overnight at 4°C, and stained with the secondary antibodies for 2 hours (Thermo Fisher Scientific, A21434 and A21245). The same protocol was used to stain for NLRP3 (Abcam, ab4207) and caspase-1 (Millipore, AB1871; secondary antibodies, Thermo Fisher Scientific, A-11055 and A-31573). iNOS staining was performed on formalin-fixed tissue and permeabilized using 0.05% Tween and 1% Triton X-100, followed by incubation with a conjugated iNOS antibody (Abcam, Ab209027) incubated overnight at 4°C. Collagen content was determined by Picrosirius Red (Abcam) staining as previously done (41). A Hamatsu NanoZoomer 2.0 was used to obtain images of NETs and iNOS staining; a Leica SP_5Confocal Microscope was used to obtain images of NLRP3 and caspase-1 staining. Collagen was visualized using polarized light microscopy (Zeiss Axio Observer). ImagePro Plus 7.0 software was used to determine plaque, $CD68^+$, collagen, and necrotic core areas. NET^+ area, $NLRP3^+$, $caspase\text{-}1^+$, and $iNOS^+$ cells were determined using ImageJ 1.51r (NIH). These data were then divided by the plaque area of the section to get the percentage positive for NETs or CD68. NET^+ macrophages were calculated by dividing the percentage of CD68 by the percentage of NETs. $NLRP3^+$, $caspase\text{-}1^+$, and $iNOS^+$ cells were divided by total cells (DAPI nuclear staining) to get the percentage of total cells.

Cholesterol crystal images were acquired using an Axioscan microscope (Carl Zeiss) using a 10× air objective. Cholesterol crystal images were captured using polarized light and are represented as the percentage of plaque area.

Laser capture microscopy and RNA-seq. $CD68^+$ cells were selected from plaques by LCM as previously described (42), and all LCM procedures were performed under RNase-free conditions. Briefly, aortic root sections were stained with H&E, and foam cells were identified and imaged with, respectively, a Leica DM-6000B microscope and Leica LMD CC7000 camera (Leica Microsystem) and verified by positive CD68 staining. Following LCM, RNA was isolated using the PicoPure Kit (Molecular Devices Inc.) and treated with DNase, and the quality and quantity were determined using an Agilent 2100 Bioanalyzer. RNA was amplified (Automated Nugen Ovation Trio Low Input RNA [500 pg]) and sequenced (HiSeq 4000 Paired-End, Illumina), and sequencing results were analyzed using Ingenuity Pathway Analysis (IPA; Qiagen). Cutoffs of –0.5 to 0.5 $\log_2$ fold change yielded 7337 analyses-ready molecules of which 4046 were downregulated and 3291 upregulated in NET^+ versus NET^- areas. The data discussed in this report have been deposited in NCBI's Gene Expression Omnibus (43) (GEO GSE145200, https://www.ncbi.nlm.nih.gov/geo/query/acc.cgi?acc = GSE145200).

To obtain transcripts of BMDMs, bone marrow cells were isolated by flushing cells from the femurs and tibiae of wild-type C57BL6 mice. Cells were differentiated into BMDMs in 4.5 g/L glucose DMEM (Lonza) with 20% FBS, 1% penicillin/streptomycin (Gibco), and murine M-CSF (10 ng/mL; PeproTech, 315-02) at 37°C and 5% CO_2 for 7 days. Cells were lysed with Buffer RLT (Qiagen) containing 10 % β-mercaptoethanol, and the Norgen Animal Tissue RNA Purification Kit (Norgen Biotek, 25700) was used to isolate RNA from cells. The Dynabeads mRNA Direct Purification Kit (Thermo Fisher Scientific, 61011) was used to isolate mRNA transcripts using Poly-A selection, and

cDNA synthesis was performed using SuperScript II Reverse Transcriptase (Thermo Fisher Scientific, 18064014). Libraries were prepared from 50 ng of each cDNA sample using the Nextera DNA library prep kit (Illumina, FC-121-1031). Samples were sequenced on the Illumina HiSeq 2000 using 50 paired-end reads.

In the case of VSMCs, cells were prepared from wild-type C57BL6 mice as in ref. 44, and the RNA was isolated and sequenced as described above.

Statistics. Data are expressed as mean ± SEM. Data were tested for normality and equal variance and analyzed by the appropriate parametric or nonparametric test (including unpaired 2-tailed *t* test, 1-way ANOVA with Tukey's multiple comparison test, and 1-way ANOVA with Dunnett's multiple comparison test) in GraphPad Prism 7, as stated in each figure. $P \leq 0.05$ was considered significant.

Study approval. All procedures were conducted under a protocol approved by the New York University Animal Care and Use Committee (160725, Creating glucose-responsive cardiovascular complications in the mouse).

Author contributions

TJ, TJB, and EAF designed experiments. TJ and TJB performed the experiments and analyses. EJB assisted with the RNA-Seq analyses. AQ helped with the analysis performed in Figure 2. XW and JA performed cholesterol crystal visualization and quantification. MV added BMDM sequencing data. TJ, TJB, JA, and EAF wrote and edited the manuscript.

Acknowledgments

We appreciate the technical contributions of Yoscar Ogando and Felix Zhou. The RNA-Seq was performed by the Genome Technology Center, a shared resource that is partially supported by Cancer Center Support Grant P30CA016087 at the Laura and Isaac Permutter Cancer Center. Funding was provided by the American Heart Association (18PRE33990436, to TJ; 18CDA34110203AHA, to TJB; and 16SDG27550012, to JA), the American Society of Hematology (18-A0-00-1001884, to TJB), and the NIH (R01 HL147252, to JA, and R01 DK095684, R01 HL117226, R01 HL084312, R01 HL129433, P01 HL092969, and P01 HL131481 to EAF, TJ, and TJB).

Address correspondence to: Edward A. Fisher, NYU School of Medicine, New Science Building 705, 435 East 30th Street, New York, New York 10016, USA. Phone: 212.263.6636; Email: edward.fisher@nyumc.org.

1. Grau AJ, et al. Leukocyte count as an independent predictor of recurrent ischemic events. *Stroke*. 2004;35(5):1147–1152.
2. Sweetnam PM, Thomas HF, Yarnell JW, Baker IA, Elwood PC. Total and differential leukocyte counts as predictors of ischemic heart disease: the Caerphilly and Speedwell studies. *Am J Epidemiol*. 1997;145(5):416–421.
3. Parathath S, et al. Diabetes adversely affects macrophages during atherosclerotic plaque regression in mice. *Diabetes*. 2011;60(6):1759–1769.
4. Gaudreault N, Kumar N, Olivas VR, Eberlé D, Stephens K, Raffai RL. Hyperglycemia impairs atherosclerosis regression in mice. *Am J Pathol*. 2013;183(6):1981–1992.
5. Nagareddy PR, et al. Hyperglycemia promotes myelopoiesis and impairs the resolution of atherosclerosis. *Cell Metab*. 2013;17(5):695–708.
6. Barrett TJ, et al. Apolipoprotein AI) promotes atherosclerosis regression in diabetic mice by suppressing myelopoiesis and plaque inflammation. *Circulation*. 2019;140(14):1170–1184.
7. Distel E, et al. miR33 inhibition overcomes deleterious effects of diabetes mellitus on atherosclerosis plaque regression in mice. *Circ Res*. 2014;115(9):759–769.
8. Döring Y, Drechsler M, Soehnlein O, Weber C. Neutrophils in atherosclerosis: from mice to man. *Arterioscler Thromb Vasc Biol*. 2015;35(2):288–295.
9. Van Avondt K, Maegdefessel L, Soehnlein O. Therapeutic targeting of neutrophil extracellular traps in atherogenic inflammation. *Thromb Haemost*. 2019;119(4):542–552.
10. Warnatsch A, Ioannou M, Wang Q, Papayannopoulos V. Inflammation. Neutrophil extracellular traps license macrophages for cytokine production in atherosclerosis. *Science*. 2015;349(6245):316–320.
11. Megens RT, et al. Presence of luminal neutrophil extracellular traps in atherosclerosis. *Thromb Haemost*. 2012;107(3):597–598.
12. Quillard T, Araújo HA, Franck G, Shvartz E, Sukhova G, Libby P. TLR2 and neutrophils potentiate endothelial stress, apoptosis and detachment: implications for superficial erosion. *Eur Heart J*. 2015;36(22):1394–1404.
13. Castanheira FVS, Kubes P. Neutrophils and NETs in modulating acute and chronic inflammation. *Blood*. 2019;133(20):2178–2185.
14. Brinkmann V, et al. Neutrophil extracellular traps kill bacteria. *Science*. 2004;303(5663):1532–1535.
15. Qi H, Yang S, Zhang L. Neutrophil extracellular traps and endothelial dysfunction in atherosclerosis and thrombosis. *Front Immunol*. 2017;8:928.
16. Soehnlein O, et al. Neutrophil secretion products pave the way for inflammatory monocytes. *Blood*. 2008;112(4):1461–1471.
17. Soehnlein O, Ortega-Gómez A, Döring Y, Weber C. Neutrophil-macrophage interplay in atherosclerosis: protease-mediated

cytokine processing versus NET release. *Thromb Haemost*. 2015;114(4):866–867.
18. Knight JS, et al. Peptidylarginine deiminase inhibition reduces vascular damage and modulates innate immune responses in murine models of atherosclerosis. *Circ Res*. 2014;114(6):947–956.
19. Borissoff JI, et al. Elevated levels of circulating DNA and chromatin are independently associated with severe coronary atherosclerosis and a prothrombotic state. *Arterioscler Thromb Vasc Biol*. 2013;33(8):2032–2040.
20. Rodondi N, et al. Markers of atherosclerosis and inflammation for prediction of coronary heart disease in older adults. *Am J Epidemiol*. 2010;171(5):540–549.
21. Armitage J, Bowman L. Cardiovascular outcomes among participants with diabetes in the recent large statin trials. *Curr Opin Lipidol*. 2004;15(4):439–446.
22. Nicholls SJ, et al. Effect of diabetes on progression of coronary atherosclerosis and arterial remodeling: a pooled analysis of 5 intravascular ultrasound trials. *J Am Coll Cardiol*. 2008;52(4):255–262.
23. Menegazzo L, et al. NETosis is induced by high glucose and associated with type 2 diabetes. *Acta Diabetol*. 2015;52(3):497–503.
24. Wong SL, et al. Diabetes primes neutrophils to undergo NETosis, which impairs wound healing. *Nat Med*. 2015;21(7):815–819.
25. Rodríguez-Espinosa O, Rojas-Espinosa O, Moreno-Altamirano MM, López-Villegas EO, Sánchez-García FJ. Metabolic requirements for neutrophil extracellular traps formation. *Immunology*. 2015;145(2):213–224.
26. de Ferranti SD, et al. Type 1 diabetes mellitus and cardiovascular disease: a scientific statement from the American Heart Association and American Diabetes Association. *Circulation*. 2014;130(13):1110–1130.
27. Ibrahim M, et al. Global status of diabetes prevention and prospects for action: A consensus statement. *Diabetes Metab Res Rev*. 2018;34(6):e3021.
28. Barrett TJ, Murphy AJ, Goldberg IJ, Fisher EA. Diabetes-mediated myelopoiesis and the relationship to cardiovascular risk. *Ann N Y Acad Sci*. 2017;1402(1):31–42.
29. Buck MD, Sowell RT, Kaech SM, Pearce EL. Metabolic Instruction of Immunity. *Cell*. 2017;169(4):570–586.
30. Rong JX, Shapiro M, Trogan E, Fisher EA. Transdifferentiation of mouse aortic smooth muscle cells to a macrophage-like state after cholesterol loading. *Proc Natl Acad Sci USA*. 2003;100(23):13531–13536.
31. Feil S, et al. Transdifferentiation of vascular smooth muscle cells to macrophage-like cells during atherogenesis. *Circ Res*. 2014;115(7):662–667.
32. Allahverdian S, Chehroudi AC, McManus BM, Abraham T, Francis GA. Contribution of intimal smooth muscle cells to cholesterol accumulation and macrophage-like cells in human atherosclerosis. *Circulation*. 2014;129(15):1551–1559.
33. Shankman LS, et al. KLF4-dependent phenotypic modulation of smooth muscle cells has a key role in atherosclerotic plaque pathogenesis. *Nat Med*. 2015;21(6):628–637.
34. Rahman K, et al. Inflammatory Ly6Chi monocytes and their conversion to M2 macrophages drive atherosclerosis regression. *J Clin Invest*. 2017;127(8):2904–2915.
35. Fuchs TA, et al. Novel cell death program leads to neutrophil extracellular traps. *J Cell Biol*. 2007;176(2):231–241.
36. Duewell P, et al. NLRP3 inflammasomes are required for atherogenesis and activated by cholesterol crystals. *Nature*. 2010;464(7293):1357–1361.
37. Pertiwi KR, et al. Neutrophil extracellular traps participate in all different types of thrombotic and haemorrhagic complications of coronary atherosclerosis. *Thromb Haemost*. 2018;118(6):1078–1087.
38. Jorch SK, Kubes P. An emerging role for neutrophil extracellular traps in noninfectious disease. *Nat Med*. 2017;23(3):279–287.
39. Miller LS, et al. MyD88 mediates neutrophil recruitment initiated by IL-1R but not TLR2 activation in immunity against Staphylococcus aureus. *Immunity*. 2006;24(1):79–91.
40. Westerterp M, et al. Cholesterol efflux pathways suppress inflammasome activation, netosis, and atherogenesis. *Circulation*. 2018;138(9):898–912.
41. Yuan C, et al. Human aldose reductase expression prevents atherosclerosis regression in diabetic mice. *Diabetes*. 2018;67(9):1880–1891.
42. Trogan E, Choudhury RP, Dansky HM, Rong JX, Breslow JL, Fisher EA. Laser capture microdissection analysis of gene expression in macrophages from atherosclerotic lesions of apolipoprotein E-deficient mice. *Proc Natl Acad Sci USA*. 2002;99(4):2234–2239.
43. Edgar R, Domrachev M, Lash AE. Gene Expression Omnibus: NCBI gene expression and hybridization array data repository. *Nucleic Acids Res*. 2002;30(1):207–210.
44. Vengrenyuk Y, et al. Cholesterol loading reprograms the microRNA-143/145-myocardin axis to convert aortic smooth muscle cells to a dysfunctional macrophage-like phenotype. *Arterioscler Thromb Vasc Biol*. 2015;35(3):535–546.